Journal of Magnetism and Magnetic Materials 432 (2017) 102–105

Contents lists available at ScienceDirect

Journal of Magnetism and Magnetic Materials

journal homepage: www.elsevier.com/locate/jmmm

Theoretical investigation of magnetic properties in interfaces of magnetic nanoparticles and amorphous carbons

Shih-Jye Sun [a,*], Hua-Shu Hsu [b], Sergei Ovchinnikov [c], Guan-Long Chen [a]

[a] Department of Applied Physics, National University of Kaohsiung, Kaohsiung 811, Taiwan
[b] Department of Applied Physics, National Pingtung University, Pingtung 900, Taiwan
[c] Kirensky Institute of Physics, Federal Research Center KSC SB RAS, Krasnoyarsk 660036, Russia

ARTICLE INFO

Article history:
Received 27 May 2016
Received in revised form 11 January 2017
Accepted 1 February 2017
Available online 3 February 2017

ABSTRACT

Based on the experimental finding of the exchange bias in amorphous carbon samples with embedded Co nanoparticles and on the graphited character of the amorphous carbon interface confirmed by molecular dynamics simulations we have proposed the interface of graphited carbon to be antiferromagnetic. A theoretical model, which comprises the Kondo interactions in the interfaces of Co nanoparticles and the induced antiferromagnetic interactions in the graphited carbons, is employed to evaluate the ferromagnetism of the interfaces of Co nanoparticles. We have shown that the ferromagnetism of interfaces of Co nanoparticles will be enhanced by the increase of antiferromagnetic interaction as well as the increase of electron density in the graphited carbons. In particular, we found that the antiferromagnetic interactions in graphited carbons will change the spin-wave excitation in interfaces of Co nanoparticles from the quasiacoustic mode to the quasioptical one.

1. Introduction

Magnetic metals, e.g., cobalt or iron, exhibit ferromagnetism in bulks as well as in nanoparticles [1–3]. However, the ferromagnetic properties appear different in diverse scales [4,5]. In particular, magnetic nanoparticles, possessing significant surface effect, represent different magnetic properties from the bulk [6,7] and even represent superparamagnetism [8,9]. If the metallic nanoparticles contact with other materials, a strong charge exchange is expected to occur through the interfaces [10,11]. Besides, the experiments and related theoretical calculations have confirmed that when metallic nanoparticles are embedded in amorphous carbon, the sp^2 orbits of carbon near the interfaces will appear dominant [12], namely, the interfaces of amorphous carbons are graphited. Therefore, the graphited carbons (GC) become conductive and the conduction electrons of GC couple with the magnetic spins of Co atoms on the interfaces of nanoparticles (CIN). In particular, a clear exchange bias was observed in the thermally annealed amorphous carbon films as Co nanoparticles are embedded in [13]. Specifically, the exchange bias will occur under both of two conditions, including the coupling interfaces between ferromagnetic (FM) and antiferromagnetic (AFM) materials and the critical temperature of FM is higher then the critical temperature of AFM [14,15]. Since interior Co nanoparticles are supposed to be superparamagnetic and CIN is ferromagnetic, these two phenomena explicitly imply that GC would become AFM after thermal annealing.

Basing on the experimental results, we intend to construct a theoretical model to calculate the magnetization of CIN as a function of magnetic coupling. Due to this coupling of CIN the essentially paramagnetic state in GC will be transferred to be AFM. We supposed that the magnetic transformations arise from the CIN bringing strong Coulomb interactions into GC as Co atoms approach C atoms through this thermal motion. Meanwhile, the ground state of a system with strong Coulomb interaction is apt to be AFM for reducing Coulomb energy via spin carriers that hop in second-order perturbations. Besides, while CIN approaches GC, a strong Kondo interaction between them arises and causes the conduction carriers of GC to possess a certain degree of localization. Specifically, CIN interacts with GC and the magnetic interactions between conduction carriers of GC are AFM as well. It is worth mentioning that the conduction carriers of GC are almost localized, yet still possess a certain degree of freedom of conduction to achieve Kondo interactions [16,17]. Since these carriers of GC are almost localized, the hopping integrals of GC carriers are less than those of graphene carriers. Essentially, the magnetization of CIN is induced by the RKKY-like interactions via the second-order of Kondo interactions [18–21], where the conduction carriers of GC are medium. In particular, the property of spin-wave excitation in CIN was investigated in this study. We found that

* Corresponding author.
E-mail address: sjs@nuk.edu.tw (S.-J. Sun).

http://dx.doi.org/10.1016/j.jmmm.2017.02.001
0304-8853/

the spin-wave excitations are dramatically changed by the magnetic coupling of GC, which will change the original acoustic mode into the optical mode, as the magnetic coupling turns on.

2. Theory description

In our model, the magnetism in the interior of Co nanoparticle is superparamagnetic which will not contribute to magnetic interactions in CIN and GC. The interactions of the carriers between CIN and GC as well as those in GC are AFM. The Hamiltonian of the model can be written as,

$$H = H_0 + H_K + H_J \tag{1}$$

H_0 is the conduction band of graphited carbon. For simplicity, we set the structure of graphited carbon identical to graphene pattern. The formula of H_0 is,

$$H_0 = \sum_{k,\sigma} \epsilon_k c^+_{k,\sigma} c_{k,\sigma} \tag{2}$$

ϵ_k is the dispersion of conduction band of GC in the momentum k representation; σ is the spin index of conduction carriers and their creation and annihilation operators are c^+ and c, respectively. The band dispersion ϵ_k derived from the hopping integral t and the dispersion factor of graphene, $\gamma_k = \left(1 + 4cos\left(\frac{\sqrt{3}}{2}k_x\right)cos\left(\frac{k_y}{2}\right) + 4cos\left(\frac{k_y}{2}\right)^2\right)^{\frac{1}{2}}$, can be written as $\epsilon_k = \pm t\gamma_k$.

H_K, which represents the Kondo interactions between the CIN and the conduction carriers of GC, is written as,

$$H_K = J_k c \sum_i S_i \cdot \sigma_i, \tag{3}$$

where J_k is the antiferromagnetic Kondo coupling between the magnetic moment, S, of CIN and the spin, σ, of conduction carriers of GC. The constant c represents the density of magnetic local moment at each carbon site and i is the site index. H_J, induced by Coulomb interactions of CIN which represents the antiferromagnetic interactions between the spins of conduction carriers of GC, which can be written as,

$$H_J = J \sum_{ij} \sigma_i \cdot \sigma_j, \tag{4}$$

where J is the antiferromagnetic coupling and σ_i represents the spin of conduction carriers at carbon site i. In order to calculate the expectation value of magnetic moment of CIN, m ($\langle S_z \rangle$), the Green function theory was employed. Subsequently, the spin-wave dispersion of CIN can be obtained as well. Eventually, the spin-wave dispersion can be written in the form,

$$\omega(|q|) = -\delta_p J_k \langle \sigma_z \rangle + \frac{1}{2} c^2 J_k \sum_p \frac{B(q)}{A(q)}. \tag{5}$$

$\omega(|q|)$, is the spin-wave dispersion as a function of momentum q ($|q|$ is the magnitude of q), which needs to be solved selfconsistently because $A(q)$ also has the function of $\omega(|q|)$; $B(q)$ and $A(q)$ in Eq. (5) respectively are, $B(q) = \langle c^+_{p+|q|,\uparrow} c_{p+|q|,\uparrow} \rangle - \langle c^+_{p,\downarrow} c_{p,\downarrow} \rangle$ and $A(q) = \omega(|q|) - \epsilon_{p,\downarrow} + \epsilon_{p+|q|,\uparrow} + 6J\langle \sigma_z \rangle - J\gamma_q \sum_{p'} (\langle c^+_{p'+|q|,\uparrow} c_{p'+|q|,\uparrow} \rangle - \langle c^+_{p',\downarrow} c_{p',\downarrow} \rangle)$; σ_z is the expectation value of magnetic moment of conduction carriers of graphited carbon; γ_q is the dispersion factor; the spin dependent band dispersion can be written in the form, $\epsilon_{p,\sigma} = \epsilon_p + \sigma J_k m$. As the spin-wave dispersion is obtained in accordance with the expectation value of magnetic moment of CIN, m can be calculated by means of Callen's formula,

$$m = \left([S - \Phi(S)][1 + \Phi(S)]^{2S+1} + [S + 1 + \Phi(S)][\Phi(S)]^{2S+1} \right) / \left([1 + \Phi(S)]^{2S+1} - [\Phi(S)]^{2S+1} \right). \tag{6}$$

$\Phi(S)$ called as magnon number function can be written as $\Phi(S) = \sum_{|q|} \frac{1}{(exp(\beta\omega(|q|)) - 1)}$ and β is the inverse of temperature energy, $\beta = \frac{1}{k_B T}$. In our model the J is less than J_k because Co is a strongly magnetic element while the antiferromagnetic coupling J is the second-order parameter of interaction. As a result, even though conduction carriers of GC are antiferromagnetically interacting with CIN, there is still magnetization σ_z at small value over these carriers of GC.

3. Results and discussions

In order to investigate the influences onto the ferromagnetism of CIN from both magnetic interactions, one of them needs to be fixed. Fig. 1(a) represents the results that the ferromagnetism of CIN increases with J_k and the larger J enhances the ferromagnetism as well. The former result is caused by the increase of Kondo screening by the increase of J_k, which attracts more conduction electrons as the medium carriers to induce ferromagnetism. The later result is caused by the fact that the medium electrons can promote the second-order perturbation motions via the increase of J, then enhance the carrier medium effect to increase the magnetism as well. Besides, in Fig. 1, the magnetization jumps as J_k is larger than a critical value. This jump arises from the competition between both interactions at the interface, namely, these antiferromagnetically interacting conduction electrons of CG near FM spins of Co will involve the spin frustrations. Fig. 1(b) presents the fact that the magnetization as a function of J is linear for small J_k and the linearity will be destroyed as J_k increases. The deviation

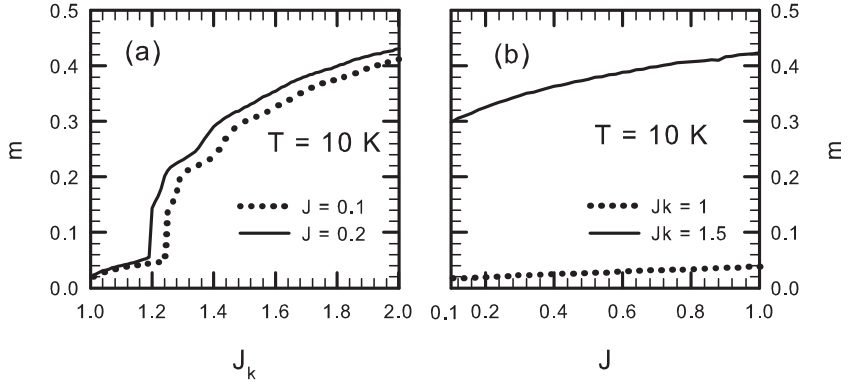

Fig. 1. The magnetization of CIN as a function of (a) J_k and (b) J at the temperature $T = 10$ K and the effective ratio of Kondo interaction $\delta_p = 0.1$.

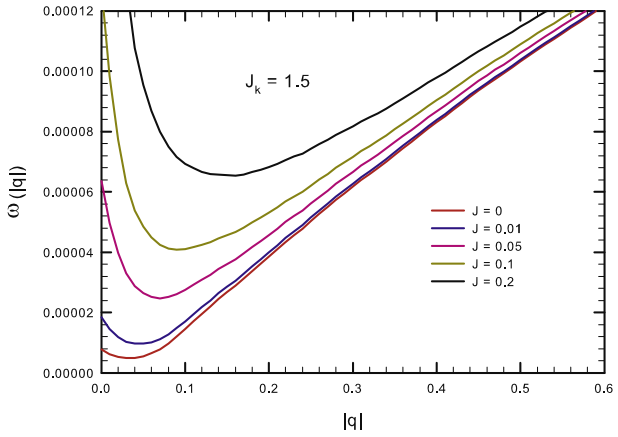

Fig. 2. The spin-wave excitations of CIN as a function of momentum $|q|$ in different J at $J_k = 1.5$ and the temperature $T = 10$ K. The cross mark in each curve represents a critical $|q|^*$, where the mode of spin waves changes from acoustic to optical as $|q|$ decreases.

of the linearity is caused by the increase of spin frustrations as aforementioned.

Fig. 2 represent the spin-wave excitations of CIN for various J. Obviously, the modes of spin waves make changes in accordance with different J. Roughly, in the most of the Brillouin zone at $q > 0.1$ the dispersion is linear for small J looking like the acoustic mode and gradually changes to the optical type of dispersion with increasing J. Nevertheless the $q \to 0$ behavior proves that the excitation gap presents for all values of J. That is why the proper terms should be quasiacoustic and quasioptical spin waves. The optical mode of spin wave is induced by a finite FM existing in CG which causes the spin frustrations. Causally, the spin frustrations destroy coherent motions of acoustic waves. Since the exchange bias can also be observed in the thermally annealed samples, the thermal motion evidently changes the spin-wave excitations in CIN. We also intend to comment this result from the symmetry point of view. The nonzero term $\langle\sigma_z\rangle$, induced by the exchange coupling, makes the symmetry decrease from a spherical to the cylindrical. It is equivalent to the effective magnetic field that provides the finite ferromagnetic resonance frequency $\omega(q = o)$. The value $\omega(q = 0)$ is proportional to the exchange coupling J. When $\langle\sigma_z\rangle$ is approaching to zero, the spherical symmetry is restored and the optical spin wave mode is transformed into acoustical one with $\omega(q = o)$=0 in agreement with the Goldstone theorem.

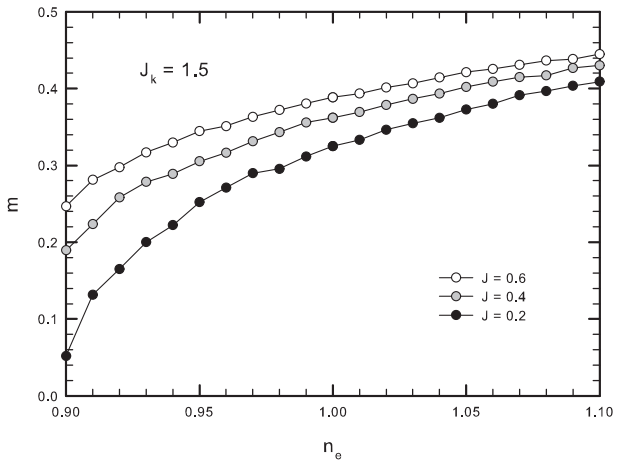

Fig. 3. The magnetization as a function of carrier density n_e of GC in various J. The interaction $J_k = 1.5$ and the temperature $T = 10$ K.

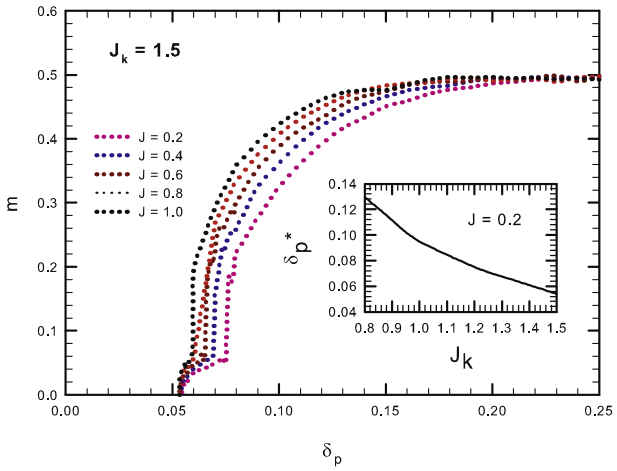

Fig. 4. The magnetization as a function of an effective ratio of Kondo interaction δ_p in various J. The interaction $J_k = 1.5$ and the temperature $T = 10$ K. The inset of the figure represents the critical δ_p as a function of J_k. The critical δ_p means the appearance of shoulder.

It is expected that the charge exchange arises between GC and CIN and leads to different magnetization with different carrier densities in GC. Fig. 3 exhibits the result that the magnetization increases with carrier density n_e. The increase of ferromagnetism results from the condition that the ferromagnetism is induced through the medium carriers, and then more carrier density makes the ferromagnetism of CIN more robust. Since the ferromagnetism in the interior of Co nanoparticles is also robust, even accompanying with a robust CIN, a rather robust ferromagnetism of Co nanoparticles is expected. As aforementioned, different metallic nanoparticles embedded in amorphous carbon represent a deviation of magnetization, because the charge exchange capacity among graphited carbons is different.

The effective ratio of Kondo interaction δ_p should be considered for real cases because different thermal annealing processes yield different portions of Co atoms approaching C atoms. Fig. 4 represents the result that for different J cases above 20% effective ratios will make the magnetism saturate. Obviously, there is a cut-off δ_p^*. No magnetism occurs under δ_p^*. δ_p^* almost retains the same value for different J. Besides, each curve shows a small shoulder-like, which obviously decreases with increase of J. As aforementioned, the suppression of the shoulder by J is caused by the fact that the medium carriers appear more active, because the second-order perturbation moves in more effect as long as J increases. The inset in Fig. 4 indicates that δ_p^* acts reversely as a function of J_k for a finite J, that is, δ_p^* decreases with increase of J_k.

4. Conclusions

Since the exchange bias experiments had been observed in the thermally annealed cobalt nanoparticles embedded amorphous carbon films, the interfaces of amorphous carbon was graphited and antiferromagnetic. Accordingly, we set up a theoretical model to simulate the magnetic properties of the interfaces of Co nanoparticles. Our model comprises two interactions in terms of, (1) the Kondo interaction between Co nanoparticles and the interfaces of graphited carbons, (2) the antiferromagnetic interaction between the electrons in the interfaces of graphited carbon. The ferromagnetism of Co nanoparticles on the interfaces is induced by the medium electrons in the graphited carbons. Our theoretical results represent the fact that the magnetization of Co nanoparticles on the interfaces will be enhanced by the increase of the anti-

ferromagnetic interactions in the interfaces of graphited carbon. In particular, we found that the spin-wave excitation will change from the quasiacoustic mode to the quasioptical one, as the antiferromagnetic interaction turns on. Besides, the charge exchange in the interfaces between the Co nanoparticles and the graphited carbons changes the magnetization of interfaces.

Acknowledgement

We would like to thank the Ministry of Science and Technology, Taiwan, for the Grant No. MOST 104-2112-M-390-001 and 104-2923-M-390-001-MY3 (Shih-Jye Sun). The work is supported also by the President of Russia program of the leading scientific schools, Grant NSh-7559.2016.2.

References

[1] R.H. Kodama, J. Mag. Mag. Mater. 200 (1999) 359.
[2] C. Petit, A. Taleb, M.-P. Pileni, Adv. Mater. 10 (1998) 259.
[3] C.J. Choi, X.L. Dong, B.K. Kim, Scr. Mater. 44 (2001) 2225.
[4] Tae-Jin Park, Georgia C. Papaefthymiou, Arthur J. Viescas, et al., Nano Lett. 7 (2007) 766.
[5] W.S. Seo, H.H. Jo, K. Lee, et al., Angew. Chem. 43 (2004) 1115.
[6] A. Punnoose, H. Magnone, M.S. Seehra, J. Bonevich, Phys. Rev. B 64 (2001) 174420.
[7] Xavier Batlle, Amilcar Labarta, J. Phys. D: Appl. Phys. 35 (2002) R15.
[8] Maria Mikhaylova, Do Kyung Kim, Natalia Bobrysheva, et al., Langmuir 20 (2004) 2472.
[9] M.E. McHenry, S.A. Majetich, J.O. Artman, M. DeGraef, S.W. Staley, Phys. Rev. B 49 (1994) 11358.
[10] Claire Goldmann, Remi Lazzari, Xavier Paquez, et al., ACS Nano 9 (2015) 7572.
[11] Q. Zhou, X. Li, Q. Fan, X. Zhang, J. Zheng, Angew. Chem. 45 (2006) 3970.
[12] Hua-Shu Hsu, Ju. Shin-Pon, Shih-Jye Sun, Hsiung Chou, C.H. Chia, EPL 114 (2016) 40001.
[13] Hua-Shu Hsu, Yu-Ying Chang, Yi-Ying Chin, Hong-Ji Lin, Chien-Te Chen, Shih-Jye Sun, Sergey M. Zharkov, Chun-Rong Lin, Sergey G. Ovchinnikov, Carbon 114 (2017) 642.
[14] J. Nogués, Ivan K. Schuller, J. Mag. Mag. Meter. 192 (1999) 203.
[15] P.K. Manna, S.M. Yusuf, Phys. Rep. 535 (2014) 61.
[16] Y.Y. Chen, P.H. Huang, M.N. Ou, et al., Phys. Rev. Lett. 98 (2007) 157206.
[17] L. Fritz, M. Vojta, Rep. Prog. Phys. 76 (2013) 032501.
[18] J. Klinovaja, D. Loss, Phys. Rev. B 87 (2013) 045422.
[19] J.M. Duffy, P.D. Gorman, S.R. Power, M.S. Ferreira, J. Phys.: Condens. Matter 26 (2014) 055007.
[20] H. Lee, J. Kim, E.R. Mucciolo, G. Bouzerar, S. Kettemann, Phys. Rev. B 85 (2012) 075420.
[21] Karol Szałowski, J. Phys.: Condens. Matter 25 (2013) 166001.